Isothermal M vs. H data obtained at different temperatures using a commercial SQUID magnetometer. ΔS_m is calculated from the M-H curves using the formula,

$$\Delta S_m = \int_0^H \left[\frac{\partial M}{\partial T}\right]_H dH$$

ΔS_m is found to be positive across the first order antiferromagnetic to ferromagnetic transition (with rising T) observed in the present Ru doped $CeFe_2$ pseudo-binaries. This tells that if a magnetic field is applied adiabatically across the FOPT in the present series of alloys, the sample would undergo a reduction in temperature. On the other hand, ΔS_m is found to be negative across the second order ferromagnetic to paramagnetic transition (with rising T). The samples would therefore produce cooling during adiabatic withdrawal of magnetic field at various starting T across the second order transition. The largest magnitude of ΔS_m in the whole series of Ru doped $CeFe_2$ measured is found to be 7.16 J per kg per K, in $Ce(Fe_{0.96}Ru_{0.04})_2$, at about 60K, i.e., across the FOPT. The largest magnitude of ΔS_m across the second order transition is observed in undoped $CeFe_2$, which does not exhibit an FOPT. ΔS_m across the second order transition appears to decrease in magnitude with Ru doping. Further studies on the present series of alloys towards the quantitative estimation of adiabatic temperature changes with changing applied magnetic fields and the refrigeration capacity of the alloys in different temperature regimes is presently in progress. These along with the parallel studies on Gd_5Ge_4 being carried out in LTPL, are expected to provide substantial information in the direction of designing suitable working materials for energy efficient and environment friendly refrigerators.

(Contributed by: M. K. Chattopadhyay (maulindu@cat.ernet.in) and Meghmalhar Manekar (megh@cat.ernet.in)

L.4 Laser rapid manufacturing of colmonoy-6 bushes

Colmonoy bushes are used as guiding material in many components of Prototype Fast Breeder Reactor (PFBR). Traditionally, these bushes are made by conventional casting process. However, the indigenous non-availability of cast bushes and prohibitive cost of imported bushes necessitated the development of alternative process for their fabrications. At present, these bushes are fabricated by depositing the hard facing alloy on austenitic stainless steel rods using Gas Tungsten Arc Welding (GTAW) process followed by precision machining. However, this process is cumbersome and time consuming, as it involves many steps of conventional processing, viz. welding, machining, grinding, etc. Therefore, another process is developed using Laser Rapid Manufacturing (LRM).

LRM is the process of fabricating near net shape three-dimensional components, directly from CAD model, by multi-layer overlapped laser cladding. Using a 10 kW CW CO_2 Laser system, integrated with co-axial powder feeding unit and 3-axis laser workstation, Colmonoy-6 bushes were fabricated with this technique. The Colmonoy alloy normally has very poor cracking resistance. However, cracks were avoided by processing at an elevated temperature (673 K) and subsequent controlled cooling.

Fig. L.4.1 *Different stages showing laser rapid manufacturing of Colmonoy bush*

The LRM fabricated bushes are then machined using Cubic Boron Nitride (CBN) tools to achieve desired dimensional tolerance of H7/h6 grade and surface finish of 0.4 micron. Testing of these bushes by various characterization techniques e.g. dye-penetrate test, Ultra-sonography, micro hardness, metallographic examination, ageing experiments for 24 hours etc., confirmed their quality at par with those made by GTAW technique.

(Contributed by: A K Nath, aknath@cat.ernet.in)

L.5 Enhancement of intergranular corrosion resistance of 316(N) weld metal by laser surface resolidification

AISI type 316LN stainless steel (SS) has been developed indigenously as main structural material for 500 MWe Prototype Fast Breeder Reactor (PFBR) at Kalpakkam. Welding of type 316LN SS is to be carried out with modified

E316-15 electrodes. Welded components are often subjected to heat treatment at various stages of manufacturing cycle for providing dimensional stability, stress relieving and for restoring desired mechanical properties and corrosion resistance. Due to higher carbon content of indigenously developed welding electrode, critical cooling rates for avoiding sensitization of the welded components after solution annealing is higher than that of the base metal. It has been established earlier that a cooling rate of 65 K/h resulted in sensitization while cooling with a higher rate of 75 K/h did not cause sensitization. Slow cooling from solution annealing temperature is preferred to reduce reintroduction of residual stresses and distortion. Laser surface resolidification with modulated laser power generated a microstructure that was resistant to sensitization even when cooled at the rate of 65 K/h.

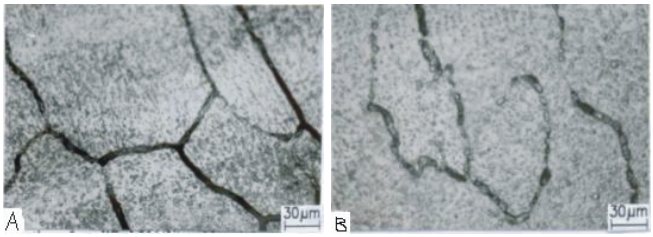

Fig. L.5.1 *Microstructures of 316 (N) weld metal after solution annealing treatment (A). Untreated base metal and (B) Laser Treated Zone.*

Laser surface treatment of modified type 316(N) weld metal were carried out with a high power CO_2 laser in CW and pulsed modes as well as with a 150 W average power pulsed Nd-YAG laser. Laser treatment conditions had a profound effect on the integrity and sensitization resistance of the treated specimen after a solution annealing treatment involving cooling at the rate of 65 K/h. Surface treated specimens with pulsed Nd-YAG laser with high peak power density and low repetition rate (3 Hz) produced numerous solidification cracks. On the other hand, surface melting with CW laser eliminated cracking but the specimens failed in intergranular corrosion (IGC) tests. However, specimens, treated with pulsed CO_2 laser at higher repetition rate (100-200 Hz) and 50% duty cycle superimposed on CW laser power (2.4kW pulses ridded over ~800W CW), not only avoided solidification cracking but also passed IGC test. In contrast to continuous grain boundary network of chromium carbide in solution-annealed base metal, fig.L.5 (A), laser surface treated region exhibited frequent discontinuities in the grain boundary network of chromium carbides, fig.L.5 (B).

(Contributed by: A K Nath, aknath@cat.ernet.in)

L.6 Improved cut quality in titanium with modulated CO_2 laser beam

Titanium finds extensive use in aerospace, medical and vacuum applications. Cutting of Titanium sheets is one of the primary requirements in the fabrication of most of the components. Non-contact laser cutting, because of its low heat input characteristics, has the capability to cut with narrow kerf width; straight cut edges, low roughness, and minimum heat affected zone (HAZ). However, initial piercing required for initiating laser cutting within the sheet and ejection of viscous molten metal for dross-free cutting usually pose problem.

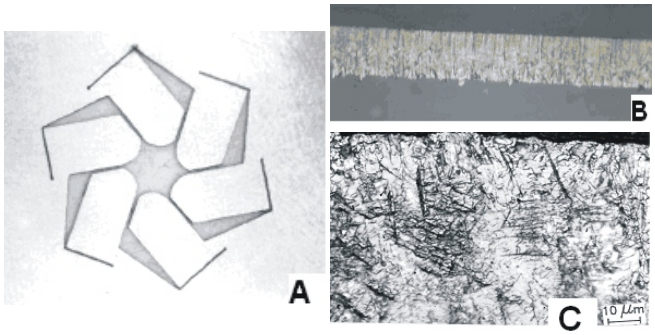

Fig. L.6.1 *A) Profile-cut Titanium sheet, B) Dross-free cut surface and C) No noticeable HAZ below cut edge. (Peak power = 600 W; frequency = 500 Hz; duty cycle = 30%, speed = 60 mm/min).*

With extensive experimental study of the dynamic behavior of melt ejection in the 1 mm thick Titanium sheet using a 3.5 kW CO_2 laser operated in continuous wave (CW) and pulsed modes and different gases e.g. Ar, He and N_2 for melt ejection, optimum laser and process parameters were established for piercing holes and dross-free profile cutting. Laser pierced holes with optimum combination of low tapering and narrow heat affected zone were created with modulated laser beam operated at high duty cycles (~80%) and Ar as shear gas for melt ejection. Dross-free cuts with no noticeable HAZ were obtained with high frequency modulated laser beam (~500 Hz) with low duty cycle (≤50%). Microscopic features of laser cut surfaces reflected the dynamic mechanism involved in laser cutting process.

(Contributed by : A K Nath, aknath@cat.ernet.in)

L.7 Characterization of magneto-optic trap

A Magneto-Optic Trap (MOT) developed for cooling and trapping of Rb atoms is shown in Fig. L.7.1. It essentially